Scientia Iranica C (2022) 29(3), 1319–1329

Sharif University of Technology
Scientia Iranica
Transactions C: Chemistry and Chemical Engineering
http://scientiairanica.sharif.edu

Study of UV-Vis absorption spectra of magnetic molecule tripyridinium bis[tetrabromidoferrate(III)] bromide with density functional formalisms

F. Baniasadi[a], M.B. Fathi[b,*], M.M. Tehranchi[a], and V. Amani[c]

a. *Department of Physics, Shahid Beheshti University, Tehran, Iran.*
b. *Department of Condensed Matter, Faculty of Physics, Kharazmi University, Tehran, Iran.*
c. *Department of Chemistry, Farhangian University, Tehran, Iran.*

Received 12 March 2021; received in revised form 5 September 2021; accepted 15 November 2021

KEYWORDS
Molecular magnet;
DFT;
TDDFT;
UV-Vis absorption spectra.

Abstract. The Ultraviolet-Visible (UV-Vis) absorption spectra of discrete magnetic molecules $[py.H]_3[FeBr_4]_2Br$ were measured based on density functional theory with B3LYP exchange-correlation functional in acetonitrile solution. The molecule was dissolved dilutely in acetonitrile to ensure that its experimental response could be attributed to a single dispersed molecule without significant interaction with other molecules. The experimental UV-Vis absorption spectra exhibited four typical peaks in the UV region and three peaks in the visible region. A number of different basis sets were employed to compare the experimental data with the theoretical absorption spectra on different levels of basis sets. The comparison between experimental data and theoretical computation demonstrated that choosing 6-311++G** improved computational results mainly in the visible region and made minor differences between the results associated with Density Functional Theory (DFT) and Time Dependent Density Functional Theory (TDDFT) in other wavelength domains, especially in UV wavelengths. The simulated results are of importance in simulating the response of these molecular magnets as a discrete asymmetric unit to applied light.

1. Introduction

A study of the electronic structure of Molecular Magnets (MM) has become a noticeable research trend owing to their interesting magneto-optical, electro-optical, and photo-magnetic properties [1–6]. In an attempt to interpret the complete map of their electronic structure, a variety of experimental and theoretical methods are proposed [7–10]. Experimentally, the electronic structures of molecules are generally elucidated using the transition and absorption spectra [11,12]. The ultraviolet-visible (UV-Vis) absorption, Ultraviolet Photoelectron Spectroscopy (UPS), and Energy Loss Spectroscopy (ELS) are almost identical methods usually justified by theoretical calculations to determine the inherent electronic structure of molecular systems [12,13].

The experimental spectroscopic data are mostly simulated by means of quantum chemistry calculations such as Hartree-Fock Configuration Interaction Single (RHF/CIS) [14], Time-Dependent Density Functional Theory (TDDFT) [14–16], and certain semi-empirical calculations via INDO or CNDO Hamiltonian [14]. Among them, TDDFT has become a widespread and popular technique to reproduce experimental spectroscopic results. This method is designed to yield the exact Excited State (ES) by means of developing the

*. *Corresponding author.*
E-mail address: fathi@khu.ac.ir (M.B. Fathi)

doi: 10.24200/sci.2021.57647.5342

Ground State (GS) with DFT formalism considering that the potentials and densities of a many-body system vary with time [13]. TDDFT alongside high-level basis sets is able to approximate the electronic transitions with a good degree of accuracy and low computational time cost [16].

The present study aims at a deeper understanding of ultraviolet and visible spectra (UV-Vis) of tripyridinium bis[tetrabromidoferrate(III)] bromide MM. Despite many theoretical attempts for electronic structure calculation of materials, the problem of finding a better approximate basis set for simulation of MMs challenges condensed-matter researchers. The line-width of absorption spectra is of critical importance for completion of simulation, even at the first-principle level. To this end, we simulate the MM of chemical formula $[py.H]_3[FeBr_4]_2Br$ via density functional approximation scheme and examine the proficiency of these methods to determine the energy levels for predicting electronic transition in this complex in some wavelength regions. This MM has been the subject of intense researches since the development of a new generation of electronic devices [17–20]. Therefore, identification of electronic transitions in these molecular complexes remains a great characterization problem since then.

This work is organized as follows: Next section is devoted to the theoretical method used for estimating absorption spectrum. Section 3 is dedicated to computational details obtained via Gaussian 2003 (A.B.3) [21–23] and Gausssum 2.2 [24]. Then, a comparison between computational results and the experimental data is made. Summary and discussion of the results are presented at the end.

2. Theoretical formulation of absorption spectra

The absorption of light by the chemical species is attributed to electronic transitions. These transitions are associated with the changes in energy among the states corresponding to the frequency variations ν, wavelength λ, and wave number of photons absorbed $\nu'(\equiv \nu)$. The absorption of light by compounds in solution is described by Bear-Lambert law [24,25].

Experimentally, the role of each energy level in electronic transitions is evaluated by the integration of all energies into the interval corresponding to the line-width via the dimensionless oscillator strength (f) for electronic transition. From the viewpoint of the transition dipole approximation, oscillator strength is estimated through electric dipole transition ($P_{i\to f}$) between initial i and final states f [26,27]:

$$f = \frac{2m_e}{3\hbar e^2}\Delta\omega_{i\to f}\left|P_{i\to f}\right|^2, \tag{1}$$

where all symbols are well known. Oscillator strength can be calculated using Gaussian function $g(x) = N.e^{-\alpha(x-\beta)^2}$ with the normalization constant N at the center of β for approximating the line-shape ε by integrating over the whole energy space. By employing the relation between α exponent and Full Width at Half Maximum (FWHM), $\Delta_{1/2}\nu = \sqrt{\frac{4\ln 2}{\alpha}}$ and $\beta = \nu_{i\to f}$, the molar absorption coefficient is obtained [28]:

$$\varepsilon(\nu) = \frac{2.175\times 10^8(\text{L.mol}^{-1}.\ \text{cm}^{-2})}{\Delta_{1/2}\nu} f\exp\left[-2.772\left(\frac{\nu-\nu_{i\to f}}{\Delta_{1/2}\nu}\right)\right]. \tag{2}$$

To compute f and $\nu_{i\to f}$, it is required to provide the ESs. The formalism of TDDFT is popular in finding time-variant dynamical quantities such as excitation energies and frequency-oriented response properties in the presence of any dynamical potentials (electric, magnetic fields, or light) [16]. In this model, the classical optical light field (electric field $\vec{E}(t)$) couples to dipole moment of atom, causing a time-dependent wave function ($\psi(\mathbf{r},t)$). This wave function can be written as a liner combination of the stationary eigenfunctions, $\psi_n(\mathbf{r})$ [28].

Upon employing time-dependent perturbation theory with linear response theory, the wave function can be obtained as follows:

$$\psi(\mathbf{r},t) = e^{-i\varepsilon_m t}\left[\psi_m(\mathbf{r}) - \sum_{n\neq m}\frac{|\mathbf{p_{mn}}|}{\hbar}\psi_m(\mathbf{r})\int\frac{d\omega}{2\pi}\frac{E(\omega)e^{-i\omega t}}{\omega+\varepsilon_{\mathbf{mn}}+i\gamma}\right], \tag{3}$$

where $\mathbf{p_{mn}}$ is the electric dipole matrix element in dipole transition approximation. The field-induced polarization, $P(t)$, is thus given by:

$$P(t) = -n_0\sum_{n\neq m}\frac{|\mathbf{p_{mn}}|^2}{\hbar}\int\frac{d\omega}{2\pi}E(\omega)e^{-i\omega t}\left[\frac{1}{\omega+\varepsilon_{mn}+i\gamma}-\frac{1}{\omega-\varepsilon_{mn}+i\gamma}\right], = \int\frac{d\omega}{2\pi}P(\omega)e^{-i\omega t}. \tag{4}$$

Since the frequency-dependent polarization, $P(\omega)$, depends on the electric field through $P(\omega) = \chi(\omega)E(\omega)$, the optical susceptibility, $\chi(\omega)$, can finally be evaluated.

The absorption coefficient $\alpha(\omega)$ can be determined by imaginary part of $\chi(\omega)$ as follows [20]:

$$\alpha(\omega) = \frac{4\pi}{n(\omega)c}\chi''(\omega), \tag{5}$$

where $n(\omega)$ is [20]:

$$n(\omega) = \sqrt{\frac{1}{2}\left(1 + 4\pi\chi'(\omega) + \sqrt{\left[1 + 4\pi\chi'(\omega)\right]^2 + \left[4\pi\chi''(\omega)\right]^2}\right)}^{1/2}. \quad (6)$$

To estimate the absorption coefficient in a complex containing many atoms, the contribution of each atom should be taken into account via molecular orbitals and their expansion coefficients [29–31]. Due to the lack of any exact solution for calculating wave function in many-body systems, various approximations employ different sets of mathematical wave functions. Molecular orbitals are nothing other than Linear Combination of Atomic Orbitals (LCAO) [32]:

$$\psi_i = \sum_{\mu=1}^{n} c_{\mu i}\varphi_\mu, \quad (7)$$

where $c_{\mu i}$ and φ_μ are the expansion coefficients and the μth atomic orbital, respectively. In Gaussian format, φ_μ is:

$$\varphi_\mu = \sum_{j=1}^{p} d_{\mu j} N_g (x - x_A)^a (y - y_A)^b (z - z_Z)^c \exp(-\alpha[(x - x_A) + (y - y_A) + (z - z_Z)]), \quad (8)$$

where α is the exponent, $d_{\mu j}$ the atomic expansion coefficient, and $r_A(x_A, y_A, z_A)$ the position of atom A; a, b, and c are the integral exponents associated with angular momentum via $L = a + b + c$.

3. Results and discussion

All calculations are performed on the computational cluster SARMAD at Shahid Beheshti University. At least, 64 cores are used through calculational processes for various different codes with different basis sets and potentials.

3.1. Tripyridinium bis[tetrabromidoferrate(III)] bromide

The formula for the molecule under study is $[py.H]_3[FeBr_4]_2Br$, which belongs to the iron tetrahaloferrate(III) group. This complex was first synthetized by Ginsberg and Robin [17]. In our previous work, we reported the abundant molecular structure of $[py.H]_3[FeBr_4]_2Br$ in acetonitrile solvent, characterized by Debye function analysis of experimental X-ray intensities [33]. The structure has been previously optimized by DFT in the scheme of B3LYP and 6-31g* approximation, and the optimized structure is reproduced in Figure 1 [33].

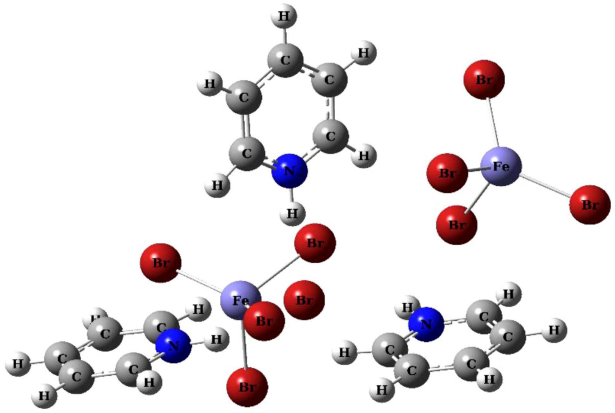

Figure 1. The plausible abundant molecular structure of $[py.H]_3[FeBr_4]_2Br$ complex in acetonitrile [33].

3.2. GS energy levels

The GS energies are calculated through the relation of the energy difference of Highest Occupied Molecular Orbital (HOMO) and Lowest Unoccupied Molecular Orbital (LUMO) $E = E_{\text{LUMO}} - E_{\text{HOMO}}$ with the absorption energy $h\nu_{i\to f}$. All calculations are done by considering acetonitrile solvent as the medium (making use of IEFPCM keyword). The DFT method with various different potentials is applied at several levels of Pople-type basis sets with or without diffuse and polarized functions. Those approximations are itemized according to the split valence basis set and diffuse function as follows: 6-31G, 6-31G*, 6-31G**, 6-31+G, 6-31+G*, 6-31+G**, 6-31++G, 6-31++G*, 6-31++G**, 6-311G, 6-311G*, 6-311G**, 6-311+G, 6-311+G*, 6-311+G**, 6-311++G, 6-311++G*, and 6-311++G**. All calculations are carried out with Gaussian 2003 (A.B.3) [14]. Table 1 lists the GS energy for different approximations in the atomic unit (1 Hartree = 27.21 eV).

According to Table 1, the calculated energies associated with 6-31+G**, 6-31++G**, 6-311+G**, and 6-311++G** were less than other calculations. These approximations are employed later.

3.3. Density of states

Density Of States (DOS) can be utilized as a valuable tool to realize transition rate or absorption spectrum. DOS demonstrates the number of states in a certain energy difference or at a given energy interval. The DOS of the isolated molecule is defined as a function of single particle energy eigenvalue (ξ) as follows:

$$DOS = \sum_i \delta(E - \xi_i). \quad (9)$$

The DOS simply takes into account Gaussian broadening function [34]. Figures 2 and 3 show this quantity for different double-zeta and triple-zeta basis sets calculated using Gausssum [23] with $FWHM = 0.2$ eV.

Table 1. Ground state energy of the molecule in different Pople basis sets in atomic units.

Basis set	Energy	Basis set	Energy
6-31G	−26418.2737096	6-311G	−26441.1486730
6-31G*	−26419.6481007	6-311G*	−26441.8209699
6-31G**	−26419.6838857	6-311G**	−26441.8565418
6-31+G	−26418.6161250	6-311+G	−26441.2998334
6-31+G*	−26419.8718641	6-311+G*	−26441.8989283
6-31+G**	−26419.9074214	6-311+G**	−26441.9336018
6-31++G	−26418.6254260	6-311++G	−26441.3014524
6-31++G*	−26419.8802820	6-311++G*	−26441.8994215
6-31++G**	−26419.915742	6-311++G**	−26441.9340157

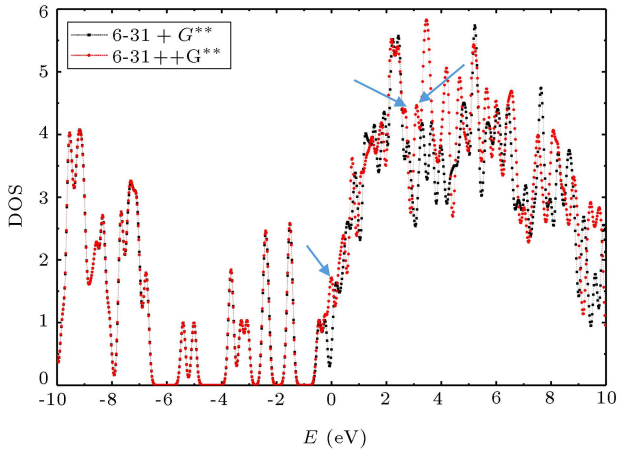

Figure 2. Calculated DOS by double-zeta basis sets: 6-31+G** and 6-31++G**.

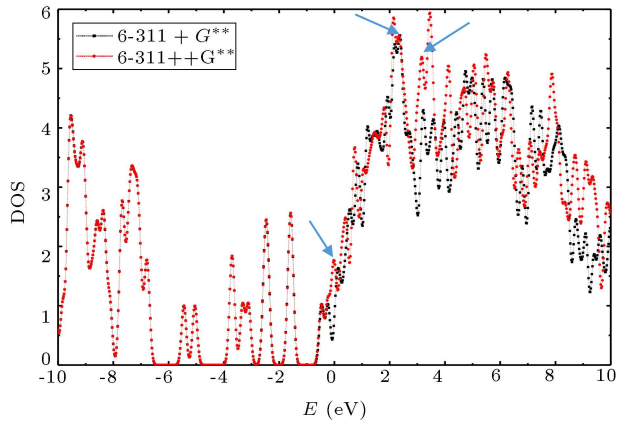

Figure 3. Calculated DOS using triple-zeta basis sets: 6-311+G** and 6-311++G**.

3.4. TDDFT simulation of absorption spectrum

Variations of MOs' energies and DOSs at different basis set levels show that they possess similar features with some difference. These differences, one of which on the Fermi surface, reflects some remarks about the adaption of basis set or approximation chosen for simulations. Based on the GS energies (Table 2), we choose 6-31++G** from the first column and 6-311++G** from the second column, since they both yield the lowest GS energy for the molecule in their categories.

DOS results represent some illuminating guidelines on the well-suited basis set for further simulation. The experimental absorption spectrum versus wavelength is shown in Figure 9. Two peaks appear at wave-lengths about $\lambda = 470, 390$ nm, which are equivalent to energies $\varepsilon \simeq 2.64, 3.2$ eV. According to Koopman's single particle picture, two corresponding electronic transitions from the Fermi level including DOSs in Figures 2 and 3 show that 6-311++G** and 6-31++G** fill the Fermi level (shown by arrows), thus allowing an electron to be transmitted to higher levels; this measure points to the most well-suited basis sets for molecule's simulation. In addition, as a rough estimate of the transition energies, these two DOSs simulated by the mentioned basis sets allow transitions to be nearly equivalent to energies at the absorption peaks, as shown by arrows.

Therefore, two basis sets 6-31++G** and 6-311++G** are applied as a benchmark for the next calculations in TDDFT studies. TDDFT calculations were performed employing G03 and the UV-Vis absorption spectra for the mentioned basis sets. The results are plotted via Gausssum package using different FWHM values (0.1, 0.2, 0.3 eV), as shown in in Figure 4.

3.5. DFT calculations employing different levels of approximation

Based on the minimum GS energy in Table 1, two basis sets including 6-31++G** and 6-311++G** are adopted for a comparative study of DFT and TDDFT and calculating electronic spectra and absorption spectrum. We determined the exponents and coefficients for the atomic orbitals and then, the molecular orbitals.

Table 2. Selected transition dipole matrix elements by 6-31++G** and 6-311++G** basis sets.

Basis set	Transition	E_{ij} (eV)	ω_{ij} ($\times 10^{15}$)	λ (nm)	$\mathbf{p}_{nm}(x,y,z)/e$ (Bohr)
6-31++G**	H→L+2	1.78	2.7043	696.54	4.2476×10^{-4}, -8.0085×10^{-3}, 3.6312×10^{-3}
	H→L+1	1.71	2.5979	725.05	1.0050×10^{-2}, -1.1033×10^{-2}, -2.3510×10^{-2}
	H-1→L	1.7	2.5828	729.32	4.8494×10^{-3}, 5.5148×10^{-2}, -5.2466×10^{-2}
	H-2→L	1.78	2.7043	696.54	3.7673×10^{-3}, 4.5497×10^{-3}, 4.5060×10^{-3}
6-311++G**	H→L+2	1.78	2.7043	696.54	5.9106×10^{-3}, 9.5928×10^{-3}, -6.3679×10^{-4}
	H→L+1	1.71	2.5979	725.05	-8.0594×10^{-3}, 1.5703×10^{-2}, 1.1932×10^{-2}
	H-1→L	1.7	2.5828	729.32	-1.2106×10^{-2}, -6.2331×10^{-2}, 6.2424×10^{-2}
	H-2→L	1.78	2.7043	696.54	-0.1092, -0.1468, 0.1835

The exponents and coefficients were obtained through single-point calculation in DFT and B3LYP by means of 'pop = full' and 'gf print' keywords. The molecular orbitals are evaluated using the outputs of calculations for the mentioned basis set. Figure 5 demonstrates the probability of finding electrons in some of these MOs.

Having the MOs for the UV-Vis transitions, the related dipole transition matrix elements $\mathbf{P}_{nm}$ can be estimated. Calculations were well carried out by means of Monte Carlo integration with errors less than $\sim 6\%$. Results of some selected transitions (HOMOs to LUMO) through the two basis sets of 6-31++G** and 6-311++G** are tabulated in Table 2.

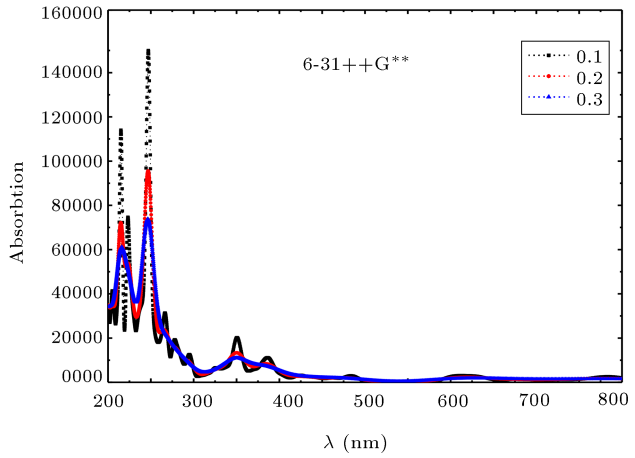

Figure 4. TDDFT simulation of absorption spectra using different FWHM values (0.1, 0.2, and 0.3 eV).

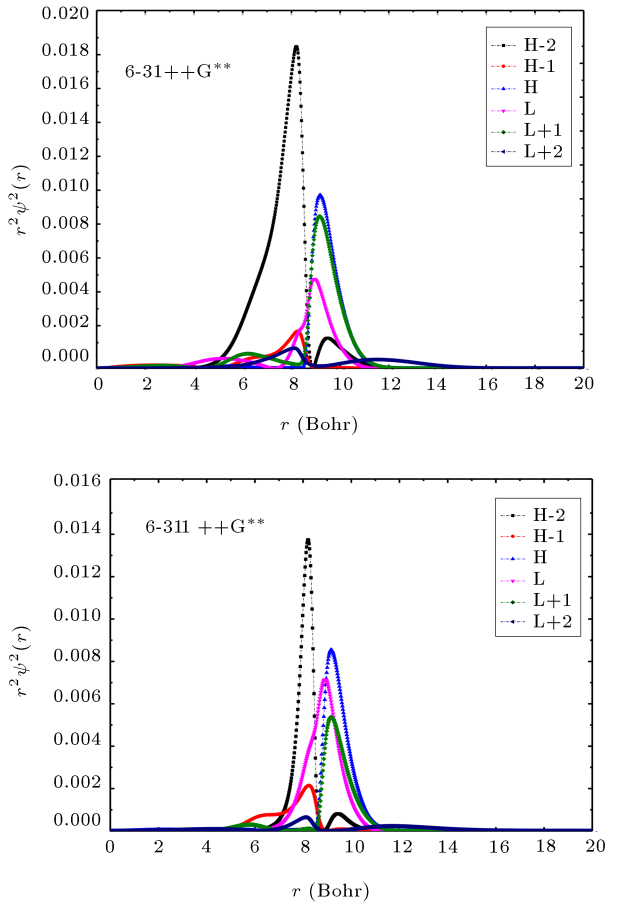

Figure 5. The probability of finding electrons in H-2, H-1, H, L, L+1, L+2.

The MOs related to the transitions in Table 2 for the basis sets 6-31++G** and 6-311++G** are shown in Figures 6 and 7, respectively.

According to the MOs in GSs (H-2, H-1, and H) and ESs (L, L+1, and L+2) in both of 6-31++G** and 6-311++G** (Figures 6 and 7), the role of pyridinium rings in absorption for the wavelengths, assumed in Table 2, can be neglected.

3.6. The refractive index

Following the calculation of the probable $\mathbf{P_{nm}}$ for transitions in the range of 300–800 nm wavelength, the refractive index $n(\omega)$ can now be calculated using Eqs. (4)–(6) through different line-widths, $\gamma = 0.1$, 0.2, 0.3 eV. The results of computations are depicted in Figure 8.

The appearance of the refractive indexes seems to have a special effect on the diagram of $\chi(\omega)$ and causes major differences in the absorption curve. The main variations appear in the magnitude of $n(\omega)$ and use of different line-widths reveals the finer structures of the curve, such that the line-width $\gamma = 0.1$ eV reveals the peaks and valleys better. Knowing the refractive index is crucial to the calculation of absorption coefficient, to be performed in the last subsection (vide infra).

3.7. The absorption coefficient

The final step is the calculation of absorption coefficient $\alpha(\omega)$. The results of these calculations help compare theoretical data with the experimental ones and to choose the well-suited basis set for approximating the experimental absorption spectrum for $[py.H]_3[FeBr_4]_2Br$ complex, measured in acetonitrile solvent. Figure 9 shows the theoretical absorption spectra alongside the experimental data.

Based on Figure 9, both of the basis sets have identical consequences outside 500–800 nm, while the size of peaks in the range of 300–600 nm significantly differs from each other. The experimental absorption spectrum for $[py.H]_3[FeBr_4]_2Br$ complex is measured in acetonitrile solvent. The theoretical calculations provide mostly the peaks; however, the places of peaks are shifted to larger wavelengths (smaller energies). These particular features of theoretical curves rely on the basics of DFT disabilities to recover the energies of ESs. The heights of peaks and valleys are comparable more suitably to the places of energies, given that the calculated strengths of oscillator for estimating dipole moment matrix are reliable in DFT scheme. In fact, the single excited electron transfer does not yield a very complicated image of the many-body correlative system in which all electrons may be excited due to single photon irradiation.

4. Summary and conclusion

The experimental absorption spectrum of the magnetic molecule tripyridinium bis[tetrabromidoferrate(III)] bromide is simulated within the scheme of density functional formalisms to decide on the best fitting procedure for simulating the experimental results using Time Dependent Density Functional Theory (TDDFT) and Density Functional Theory (DFT). As a conclusion,

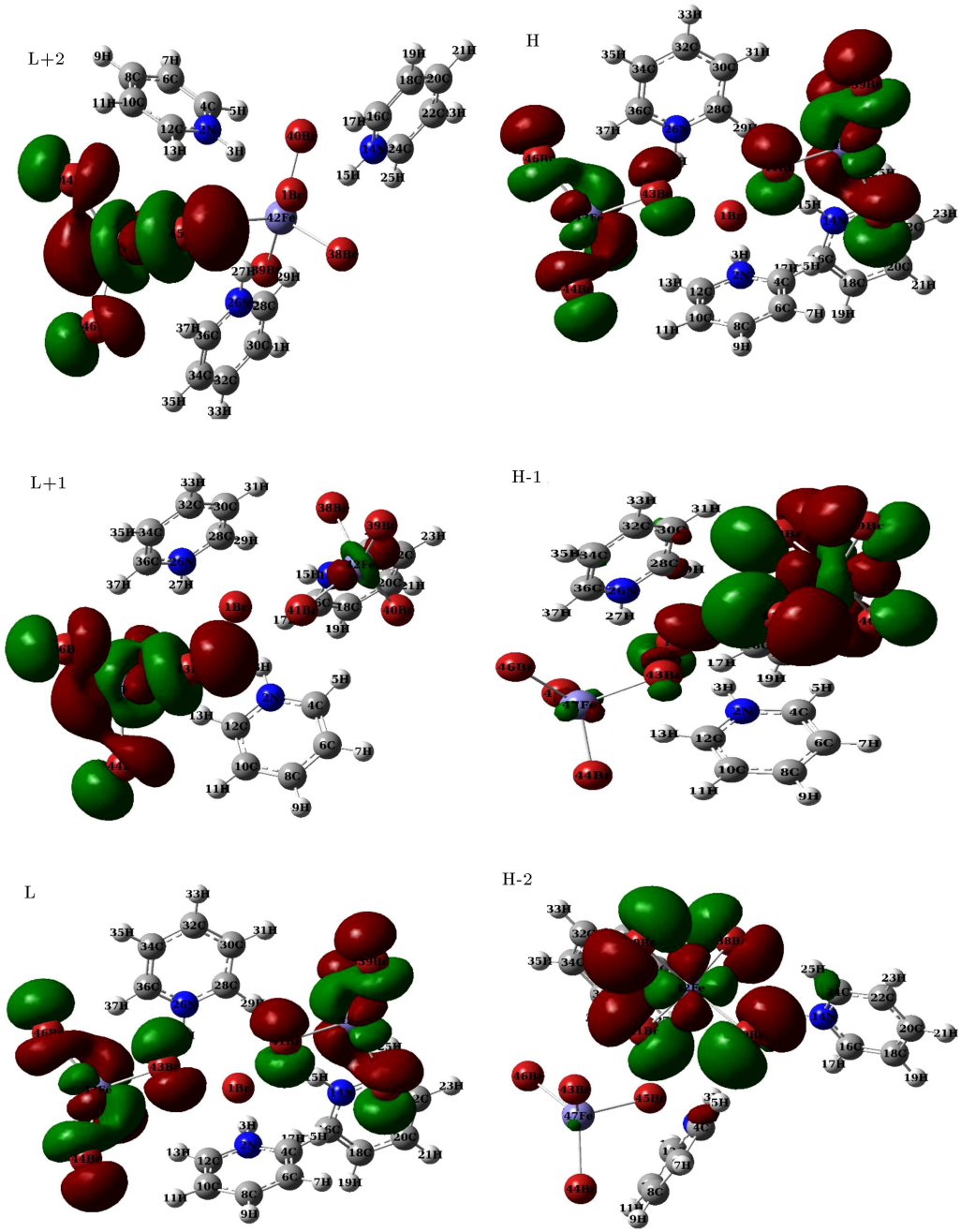

Figure 6. Selected HOMO and LUMOs using 6-31++G**.

choosing TDDFT can determine the place of peaks in the wave-length region more accurately than choosing DFT, but cannot fully estimate the strength of peaks in comparison to DFT. On the other hand, choosing DFT determines the height of peaks (i.e., the strengths of peaks) better. In addition, the theoretical results were consistent with the experimental ones concerning the most plausible line-width of the molecule about 0.1 eV.

The deviation of theoretical absorption spectra from the experimental may be attributed to: (1) neglecting pyridinium rings in Highest Occupied Molecular Orbital (HOMOs) and Lowest Unoccupied Molecular Orbital (LUMOs); (2) abilities of DFT to determine the excited states; (3) the faulty image of the single electron excited in the process of irradiation of matter with a single photon (in fact, if the measurement can be done through single electron transfer, as in the PES or ARPES experiments, the measurement will yield more compatible results by DFT). Therefore, considering single excited MOs in electron transitions may correct the energies of levels by an exciton-like transition, which includes the electron-hole Columbic interaction.

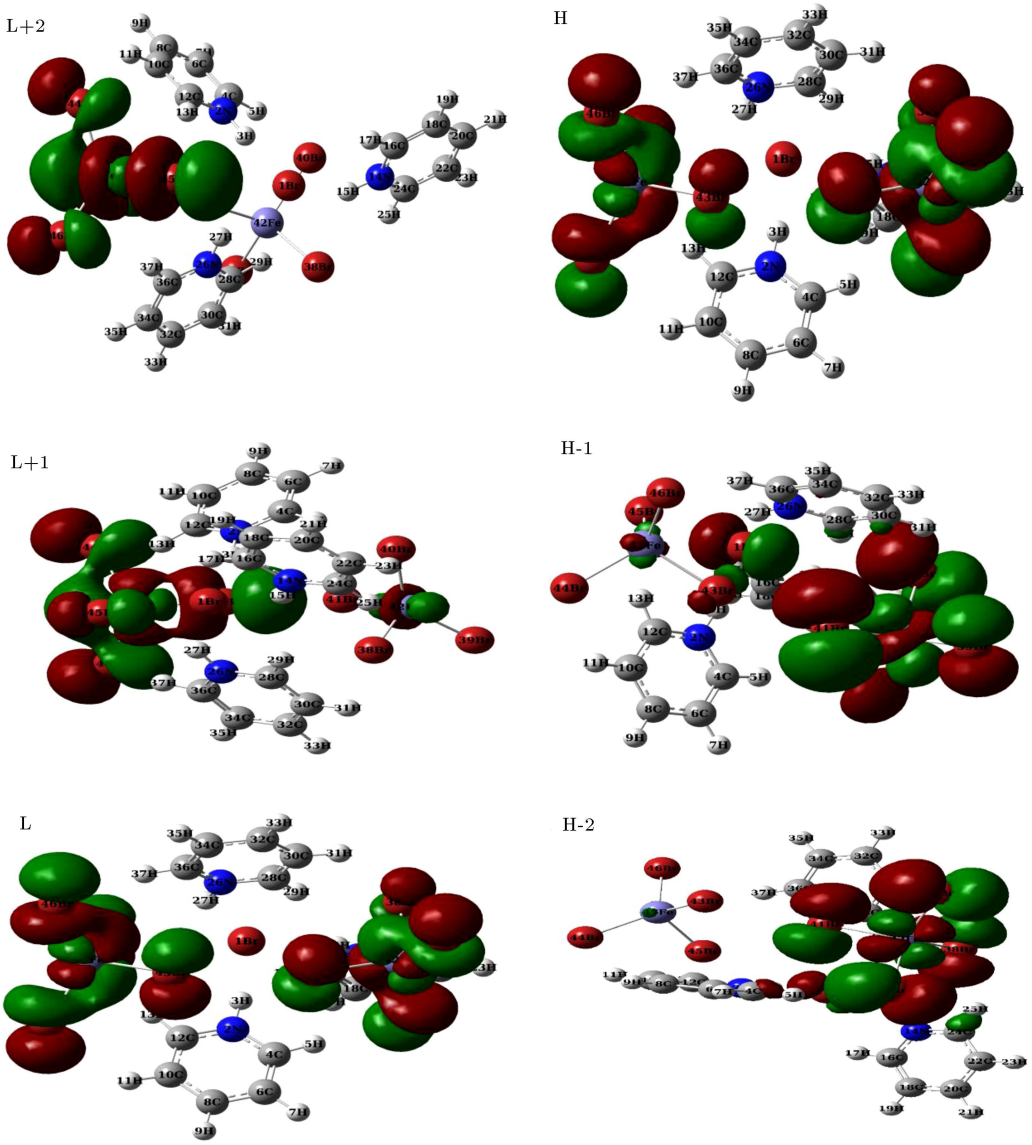

Figure 7. Selected HOMO and LUMOs using 6-311++G**.

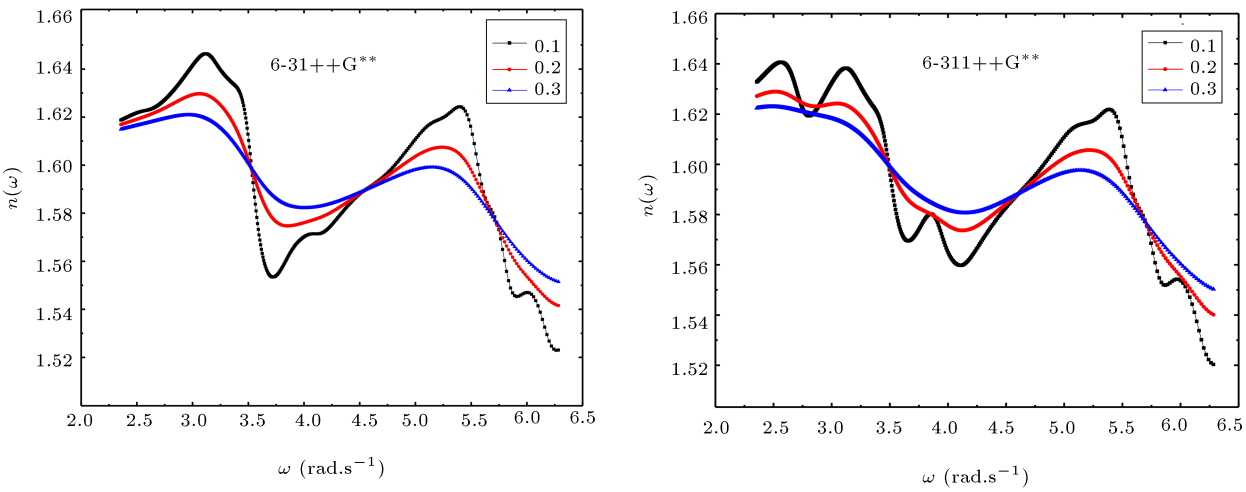

Figure 8. The refractive indexes at different line-widths (0.1, 0.2, and 0.3 eV).

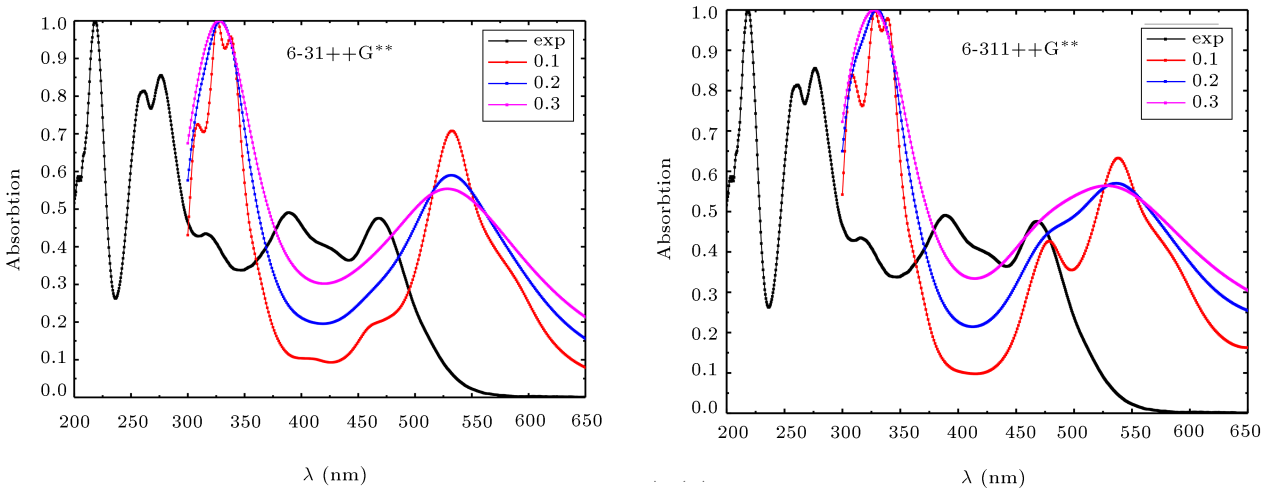

Figure 9. DFT simulation of absorption spectra at different line-widths (0.1, 0.2, and 0.3 eV) compared with the experimental data.

References

1. Ohkoshi, S-i. and Hashimoto, K. "Photo-magnetic and magneto-optical effects of functionalized metal polycyanides", *Journal of Photochemistry and Photobiology C: Photochemistry Reviews*, **2**(1), pp. 71–88 (2001).

2. Xu, Y-K., Li, H., He, B-G., et al. "Electronic structure and magnetic anisotropy of single-layer rare-earth oxybromide", *ACS Omega*, **5**(23), pp. 14194–14201 (2020).

3. Gong, C., Li, L., Li, Z., et al. "Discovery of intrinsic ferromagnetism in two-dimensional van der Waals crystals", *Nature*, **546**, pp. 265–269 (2017).

4. Sieklucka, B. and Pinkowicz, D., *Molecular Magnetic Materials: Concepts and Applications*, Wiley (2017).

5. Boukhvalov, D.W., Al-Saqer, M., Kurmaev, E.Z., et al. "Electronic structure of a Mn_{12} molecular magnet: Theory and experiment", *Phys. Rev. B*, **75**, p. 014419 (2007).

6. Carlotto, S., Sambi, M., Sedona, F., et al. "A theoretical study of the occupied and unoccupied electronic structure of high- and intermediate-spin transition metal phthalocyaninato (Pc) complexes: VPc, CrPc, MnPc, and FePc", *Nanomaterials*, **11**, p. 54 (2021).

7. Xue, Z.X., Qua, Y., Zan, Y.H., et al. "Broadening of the optical absorption spectra in ZnO nanowires induced by mixed-phase $Mg_xZn_{1-x}O$ shells", *Journal of Applied Physics*, **129**, 024502 (2021).

8. Wang, H., Li, J., Li, K., et al. "Transition metal nitrides for electrochemical energy applications", *Chem. Soc. Rev.*, **50**, pp. 1354–1390 (2021).

9. Verdaguer, M. "Rational synthesis of molecular magnetic materials: a tribute to Olivier Kahn", *Polyhedron*, **20**, pp. 1115–1128 (2001).

10. Garino, C., Borfecchia, E., Gobetto, R., et al. "Determination of the electronic and structural configuration of coordination compounds by synchrotron-radiation techniques", *Coord. Chem. Rev.*, **277–278**, pp. 130–186 (2014).

11. Anak, B., Bencharif, M., and Rabilloud, F. "Time-dependent density functional study of UV-visible absorption spectra of small noble metal clusters (Cu_n, Ag_n, Au_n, $n = 2 - 9, 20$)", *RSC Adv.*, **4**, pp. 13001–13011 (2014).

12. Pal, G., Pavlyukh, Y., Hübner, W., et al. "Optical absorption spectra of finite systems from a conserving Bethe-Salpeter equation approach", *EPJ B*, **79**, pp. 327–334 (2011).

13. Dreuw, A. and Head-Gordon, M. "Single-reference ab initio methods for the calculation of excited states of large molecules", *Chem. Rev.*, **105**, pp. 4009–4037 (2005).

14. Runge, E. and Gross, E.K.U. "Density-functional theory for time-dependent systems", *Phys. Rev. Lett.*, **52**, p. 997 (1984).

15. Rohringer, N., Peter, S., and Burgdorfer, J. "Calculating state-to-state transition probabilities within time-dependent density-functional theory", *Phys. Rev. A*, **74**(4), 042512 (2006).

16. Anouar, E.H., Osman, C.P., Frederic, J., et al. "UV/Visible spectra of a series of natural and synthesised anthraquinones: experimental and quantum chemical approaches", *Springer Plus*, **3**(233) (2014).

17. (a) Ginsberg, A.P. and Robin, M.B. "The structure, spectra, and magnetic properties of certain iron halide complexes", *Inorg. Chem.*, **2**(4), pp. 817–822 (1963). (b) Zora, J.A., Seddon, K.R., Hitchcock, P.B., et al. "Magnetochemistry of the tetrahaloferrate(III) ions. 1. Crystal structure and magnetic order-

ing in bis[4-chloropyridinium tetrachloroferrate(III)]-4-chloropyridinium chloride and bis[4-bromopyridinium) tetrachloroferrate(III)]-4-bromopyridinium chloride", *Inorg. Chem.*, **29**(18), pp. 3302–3308 (1990).
(c) Lowe, C.B., Carlin, R.L., Schultz, A.J., et al. "Magnetochemistry of the tetrahaloferrate(III) ions. 2. Crystal structure and magnetic ordering in [4-Br(py)H]$_3$Fe2Cl1.3Br7.7 and [4-Cl(py)H]$_3$Fe2Br9. The superexchange paths in the A3Fe2X9 salts", *Inorg. Chem.*, **29**(18), pp. 3308–3315 (1990).
(d) Lowe, C.B., Schultz, A.J., Shaviv, R., et al. "Magnetochemistry of the Tetrahaloferrate(III) Ions. 7. Crystal Structure and Magnetic Ordering in (pyridinium)3Fe2Br9", *Inorg. Chem.*, **33**(14), p. 3051 (1994).

18. Baniasadi, F., Tehranchi, M.M., Fathi, M.B., et al. "Intra-molecular magnetic exchange interaction in the tripyridinium bis[tetrachloroferrate(iii)] chloride molecular magnet: a broken symmetry-DFT study", *Phys. Chem. Chem. Phys.*, **17**, p. 19119 (2015).

19. Baniasadi, F., Tehranchi, M.M., Fathi, M.B., et al. "Room temperature photoinduced magnetism in [py.H]$_3$[FeCl$_4$]$_2$Cl", *Mater. Chem. Phys.*, **168**(15), pp. 35–41 (2015).

20. Fathi, M.B. and Kamalkhani, N. "The plausible superexchange pathway inside the magnetic molecule tripyridinium bis[tetrachloroferrate (III)] chloride via study of DOS and Mos", *Russian Journal of Physical Chemistry A*, **95**(2), pp. S380–S387 (2021).

21. Frisch, M.J., Trucks, G.W., Schlegel, H.B., et al., *Gaussian 03 (Revision A.1)*, Gaussian: Pittsburgh, PA (2003).

22. Schubert, K., Gua, M., Atak, K., et al. "The electronic structure and deexcitation pathways of an isolated metalloporphyrin ion resolved by metal L-edge spectroscopy", Edge Article, *Chem. Sci.*, **12**(11), pp. 3966–3976 (2021) (Advance Article).

23. O'boyle, N.M., Tenderholt, A.L., and Langner, K.M. "cclib: A library for package-independent computational chemistry algorithms", *J. Comput. Chem.*, **29**(5), pp. 839–845 (2008).

24. Valeur, B., *Molecular Fluorescence: Principles and Applications*, Digital Encyclopedia of Applied Physics-Wiley Online Library-VCH (2003).

25. Atkins, P.W. and de Paula, J., *Physical Chemistry*, 9th Ed., W H Freeman and Company (2010).

26. Atkins, P.W. and Friedman, R., *Molecular Quantum Mechanics*, Oxford University Press (2005).

27. Klessinger, M., Michl, J., *Excited States and Photo-Chemistry of Organic Molecules*, 1st Ed., VCH, New York (1995).

28. Haug, H. and Koch, S.W., *Quantum Theory of the Optical and Electronic Properties of Semiconductors*, World Scientific Publishing (2000).

29. Klán, P. and Wirzr, J., *Photochemistry of Organic Compounds*, From Concepts to Practice Wiley (2009).

30. Wang, X., Li, L., Gong, K., et al. "Modelling air quality during the EXPLORE-YRD campaign - Part I. Model performance evaluation and impacts of meteorological inputs and grid resolutions", *Atmospheric Environment*, **246**(1), p. 118131 (2021).

31. Dong, Y., Peng, W., Liu, Y., et al. "Photochemical origin of reactive radicals and halogenated organic substances in natural waters: A review", *Journal of Hazardous Materials*, **401**(5), p. 123884 (2021).

32. Atkins, P.W. and Friedman, R., *Molecular Quantum Mechanics*, Oxford University Press, Oxford, New York (2005).

33. Baniasadi, F., Sahraei, N., Fathi, M.B., et al. "X-ray characterization of tripyridinium bis[tetrabromidoferrate(III)] bromide asymmetric unit in solution by Debye function analysis", *International Journal of Modern Physics B*, **30**(24), p. 1650174 (2016).

34. Grekhov, A.M., Gun'ko, V.M., Klapchenko, G.M., et al. "Calculations of electronic structure and density of states of ideal and disordered silicon clusters", *Theor. Exp. Chem.*, **20**(4), pp. 447–451 (1984).

Biographies

Farzaneh Baniasadi was born in 1983 in Tehran and graduated from Shahid Beheshti University in December 2015 in the field of Quantum Physical Chemistry under supervision of Professor Mohamad Mehdi Tehranchi and Mohammad Bagher Fathi. Her PhD thesis involved "photomagnetism", and is entitled "Mechanism of photo induced magnetism in [py.H]$_3$[FeCl$_4$]$_2$Cl at room temperature". Study of nanoparticle by optical and statistical methods, material simulation and characterization, density functional theory calculation, and quantum optical theory constituted the main scientific topics during Baniasadi's advanced educational (MSc and PhD) courses. After the PhD program, F. Baniasadi joined Royan Institute. Now, she is a Researcher at Royan Institute (cryobiology team) and studies the synthesis of nanoparticles and their nontoxicity effect on reproduction and cryopreservation. She hopes to obtain a green nanoparticle to reduce cryopreservation side-effects. Dr. Farzaneh Baniasadi has published over 7 national and international papers and presented about 10 scientific abstracts and lectures in symposia and congresses.

Mohammad Bagher Fathi was born in Tehran, Iran. He obtained his BSc in Physics from Shahid Beheshti University in 2002, MSc in Condensed Matter Physics from Shahid Beheshti University in 2004, and PhD in Condensed Matter Physics from Sharif University of Technology in 2010. He is working on different

aspects of condensed matter theory from elementary excitations through characterization of materials. His main areas of interests are characterization of strongly correlated materials, especially during phase transitions. He has published many research articles in the national and international journals.

Mohammad Mehdi Tehranchi is an Iranian theoretical physicist and a distinguished professor at Laser and Plasma Research Institute and Department of Physics of Shahid Beheshti University. He is a member of the board of trustees and is the President of the Islamic Azad University. He was a former rector of the Islamic Azad University Central Tehran Branch and Islamic Azad University of Tehran Province and Shahid Beheshti University.

Vahid Amani received his PhD in Inorganic Chemistry in 2012 from Shahid Beheshti University. He worked as a Postdoctoral Researcher at the Department of Chemistry, University of Shahid Beheshti (2012–2015). He was a high-school Chemistry Teacher in Chahardangeh region for 16 years. In 2016, He joined the Department of Chemistry, Farhangian University in Tehran. His research interests lie in coordination chemistry, biochemistry, and chemical education. He has authored and co-authored over 230 peer-reviewed research papers.